doi:10.1093/brain/awy198 BRAIN 2018: 141; 2592–2604 | 2592

BRAIN
A JOURNAL OF NEUROLOGY

GDAP2 mutations implicate susceptibility to cellular stress in a new form of cerebellar ataxia

Ilse Eidhof,[1,*] Jonathan Baets,[2,3,4,*] Erik-Jan Kamsteeg,[1] Tine Deconinck,[2,3] Lisa van Ninhuijs,[1] Jean-Jacques Martin,[3] Rebecca Schüle,[5,6] Stephan Züchner,[7,8] Peter De Jonghe,[2,3,4] Annette Schenck,[1,#] and Bart P. van de Warrenburg[9,#]

[*,#]These authors contributed equally to this work.

Autosomal recessive cerebellar ataxias are a group of rare disorders that share progressive degeneration of the cerebellum and associated tracts as the main hallmark. Here, we report two unrelated patients with a new subtype of autosomal recessive cerebellar ataxia caused by biallelic, gene-disruptive mutations in *GDAP2*, a gene previously not implicated in disease. Both patients had onset of ataxia in the fourth decade. Other features included progressive spasticity and dementia. Neuropathological examination showed degenerative changes in the cerebellum, olive inferior, thalamus, substantia nigra, and pyramidal tracts, as well as tau pathology in the hippocampus and amygdala. To provide further evidence for a causative role of *GDAP2* mutations in autosomal recessive cerebellar ataxia pathophysiology, its orthologous gene was investigated in the fruit fly *Drosophila melanogaster*. Ubiquitous knockdown of *Drosophila Gdap2* resulted in shortened lifespan and motor behaviour anomalies such as righting defects, reduced and uncoordinated walking behaviour, and compromised flight. Gdap2 expression levels responded to stress treatments in control flies, and Gdap2 knockdown flies showed increased sensitivity to deleterious effects of stressors such as reactive oxygen species and nutrient deprivation. Thus, *Gdap2* knockdown in *Drosophila* and *GDAP2* loss-of-function mutations in humans lead to locomotor phenotypes, which may be mediated by altered responses to cellular stress.

1 Department of Human Genetics, Donders Institute for Brain, Cognition, and Behavior, Radboud University Medical Centre, 6525 GA Nijmegen, The Netherlands
2 Neurogenetics Group, Center for Molecular Neurology, VIB, 2610 Antwerp, Belgium
3 Institute Born-Bunge, University of Antwerp, 2610 Antwerp, Belgium
4 Neuromuscular Reference Centre, Department of Neurology, Antwerp University Hospital, 6520 Antwerp, Belgium
5 Department of Neurodegenerative Diseases, Hertie-Institute for Clinical Brain Research and Center of Neurology, University of Tübingen, 72076 Tübingen, Germany
6 German Center for Neurodegenerative Diseases (DZNE), 72076 Tübingen, Germany
7 Dr. John T. Macdonald Foundation, Department of Human Genetics, FL33136 Miami, USA
8 John P. Hussman Institute for Human Genomics, University of Miami, Miller School of Medicine, FL33136 Miami, USA
9 Department of Neurology, Donders Institute for Brain, Cognition, and Behavior, Radboud University Medical Centre, 6525 GC Nijmegen, The Netherlands

Correspondence to: Bart van de Warrenburg
Department of Neurology, Radboudumc
Reinier Postlaan 4
6525 GC Nijmegen, The Netherlands
E-mail: Bart.vandewarrenburg@radboudumc.nl

Correspondence may also be addressed to: Annette Schenck
Department of Human Genetics, Radboudumc

Received December 15, 2017. Revised March 9, 2018. Accepted June 11, 2018. Advance Access publication August 2, 2018

Geert Grooteplein Zuid 10
6525 GA Nijmegen, The Netherlands
E-mail: Annette.Schenck@radboudumc.nl

Keywords: autosomal recessive cerebellar ataxia; spasticity; whole exome sequencing; *Drosophila melanogaster*; cellular stress

Abbreviation: ARCA = autosomal recessive cerebellar ataxia

Introduction

The autosomal recessive cerebellar ataxias (ARCAs) are a clinically and genetically heterogeneous group of mainly degenerative diseases of the cerebellum and, often, of other central and peripheral nervous system components (Anheim *et al.*, 2012). Mutations in >100 different genes are associated with ataxia. While most of these genes are included in current diagnostic gene panels, not all ARCA patients can be genetically characterized, suggesting the existence of even more ARCA genes. Presumably, some of these yet unidentified ARCA subtypes are extremely rare or private, complicating their discovery. There is growing evidence for a convergence of molecular processes implicated in ataxias (Lim *et al.*, 2006; Smeets and Verbeek, 2014; Didonna and Opal, 2016). Further insight into these processes remains a crucial requisite when striving for targeted interventions in these currently untreatable disorders.

Here, we report mutations in *GDAP2* in patients with a new ARCA subtype and describe the corresponding neuropathology. A *Drosophila* GDAP2 model supports a role of GDAP2 in motor behaviour and suggests that cellular stress might be driving the neurodegenerative cascade.

Materials and methods

The Nijmegen (NIJ) and Antwerp (AW) sites, connected via existing European research networks on ataxia [Ataxia Study Group (ASG, www.ataxia-study-group.net) and E-rare consortium PREPARE], both initiated exome sequencing for diagnostic and research purposes in patients with (presumed) inherited ataxia. Independently, variants in *GDAP2* were identified in two unrelated ARCA patients.

Genetic testing

Both patients gave consent for further genetic testing. Exome sequencing was essentially performed as previously described (Synofzik *et al.*, 2016; van de Warrenburg *et al.*, 2016). Briefly, capture of exons was done using a SureSelect XT Human All Exon 50Mb Kit V5 (Agilent). Sequencing was performed using a Hiseq 2000 (Illumina). Read mapping and variant calling were done using BWA (http://bio-bwa.sourceforge.net/index/shtml) and GATK (https://software.broadinstitute.org/gatk/), respectively.

For proband Patient NIJ, the median target coverage was at least 75. Annotation was done using an in-house designed pipeline (Neveling *et al.*, 2013). Altogether, 117 708 variants (single nucleotide variants and small deletions/insertions/indels) were detected. Initial filtering for a gene panel of movement disorders revealed no mutations. Gene panel DGD200614 (https://issuu.com/radboudumc/docs/dgd200614_movement_disorders?e=28355229/50854884) was used. The full exome sequencing dataset was then filtered for all deletions, insertions, nonsense, and canonical splice site variants, as well as for evolutionary conserved missense variants. The data were filtered for all homozygous and compound heterozygous variants, with a frequency below 1:1000 in dbSNP, the Nijmegen exome database (>10 000 exomes), or ExAC (Exome Aggregation Consortium).

For proband Patient AW, annotation and filtering was performed using the GENESIS (gem.app) platform, a web-based tool for next generation sequencing data analysis (http://thegenesisprojectfoundation.org/) (Gonzalez *et al.*, 2013, 2015). A total of 90.8 million reads were produced for this sample, 99.93% of which could be aligned to the targeted sequence. Mean coverage of the targeted sequence was 75-fold; 90 560 single-nucleotide variations and 8961 indels were called. No obvious variants in known ataxia genes were observed. Variants were filtered for (i) non-synonymous homozygous or compound heterozygous mutations in genes that were (ii) absent or extremely rare (minor allele frequency <0.5%) in the public databases dbSNP137, NHLBI ESP6500, 1000Genomes project, and ExAC (60 706 exomes; Exome Aggregation Consortium, http://exac.broadinstitute.org/) as well as in GENESIS (<11 heterozygous or homozygous alleles in 6064 subjects in the GENESIS database); (iii) showed a rather high conservation [PhastCons score (100 vertebrate genomes) >0.75, phyloP (100 vertebrate genomes) >2]; and (iv) high genotype quality [quality filter (QUAL) >50 and genotype quality >75].

In both families, Sanger sequencing was performed for confirmation of the variants and for segregation analyses using standard techniques.

Neuropathological examination

Patient AW had given consent for a post-mortem brain examination. The neuropathological examination was conducted on paraffin sections representative of all parts of the brain. Paraffin sections were stained for cytology (Nissl, haematoxylin and eosin), and myelin (Klüver-Barrera). Immunostaining was performed using the citrate buffer epitope retrieval method. Endogenous peroxidase was quenched by incubation for 20 min at room temperature in a PBS/0.1% Triton™ X-100 (Sigma) solution containing 10% methanol and 0.003% H_2O_2. Microscope slides carrying brain sections were washed three times and incubated in the blocking solution (0.1% PBS, 4% Triton™ X-100, 4% normal goat serum, 2% bovine serum albumin) for 1 h at room temperature. Sections were then incubated for 48 h at 4°C with specific antibodies diluted in blocking solution against the following proteins: hyperphosphorylated protein tau AT8, amyloid-β 17-24 4G8, ubiquitin, TDP-43, p62,

alpha-synuclein and 1C2 against expanded polyglutamine chains. Sections were washed three times, incubated for 2 h at room temperature with the corresponding biotinylated appropriate (anti-mouse or anti-rabbit) secondary antibody (1:250; Vector Laboratories) diluted in blocking solution and washed another three times. Bound antibodies were visualized using the ABC amplification system (Vectastain ABC kit, Vector Laboratories) with 3,3′-diaminobenzidine tetrahydrochloride (DAB Metal Concentrate; Biogenex) as the substrate. The sections, nuclear-counterstained with haematoxylin or not, were dehydrated twice in ethanol and xylene solutions and mounted with Eukitt®. The lesions were semi-quantitatively assessed and estimated as severe, moderate or absent.

Flystocks and breeding

Fly stocks were maintained at room temperature on standard *Drosophila* diet (cornmeal, sugar and yeast). Crosses were maintained at 25°C, 70% humidity, 12 h light-dark cycle. The *Gdap2* RNAi lines vdrc39224 with RNAi construct 15367 (Gdap2 RNAi-1) and vdrc100622 with RNAi construct 108807 (Gdap2 RNAi-2) and their corresponding genetic control lines vdrc60000 (control-1) and vdrc60100 (control-2) were obtained from the Vienna *Drosophila* Resource Centre. The genomic insertion site of vdrc100622 was characterized by PCR as previously described and found to be at landing site 30B3, not prone to reported potential dominant phenotypes unrelated to RNAi (Green *et al.*, 2014; Vissers *et al.*, 2016). RNAi was induced with the Gal4 driver *UAS-Dicer-2;Actin-Gal4/CyO, GFP*. The original stock, #25708, was obtained from the Bloomington *Drosophila* stock centre (Indiana University) and rebalanced with CyO-GFP. For all experiments, knockdown flies were compared to their appropriate genetic background controls [progeny of the promoter line crossed with the genetic background of the vdrc GD (vdrc60000) or KK (vdrc60100) RNAi library].

Verification of *Gdap2* knockdown efficiency by quantitative PCR

To evaluate the RNAi-induced *Gdap2* knockdown efficiency, 2-day-old males of the appropriate genotypes were selected for reverse transcriptase quantitative (q)PCR. Total RNA was purified from whole bodies (five animals were used per biological replicate) and qPCR were performed as described with the following adaptations (Mukhopadhyay *et al.*, 2010). RNA was subjected to DNase treatment using the DNA-free kit (Ambion) before cDNA synthesis to avoid genomic contamination. RNA PolII (5′-CCGCGATACTTCTCTCCAC-3′ and 5′-GACCAGCTAGGCGACATTC-3′) was used as the reference gene. *Gdap2* primer sequences were 5′-AACTATCCATCGCTGCACTG-3′ and 5′-GGGGTGCACGA TATAGAAGG-3′. For each genotype, three biological and two technical replicates were analysed.

Eclosion rate and survival

For Gdap2 knockdown, homozygous Gdap2 RNAi-1 or -2 males were mated to heterozygous *UAS-Dicer-2;Actin-Gal4/CyO, GFP* virgins yielding progenies of two genotypes, the expected ratios of which provided the basis for the evaluation of the eclosion rate. For this, the number of non-*CyO, GFP Gdap2* knockdown males and *Cyo, GFP* siblings from five independent crosses was counted for five consecutive days. The experiment was repeated three times. For survival, at least 60 male flies were collected at the day of eclosion for each genotype and were subsequently aged on standard fly food. Every 2–3 days adults were transferred to vials with fresh food and dead flies were counted until all had died.

Island assay

The island assay was used to evaluate the locomotor behaviour of the 2-day-old *Drosophila* GDAP2 knockdown models as described (Schmidt *et al.*, 2012; Kochinke *et al.*, 2016; Eidhof *et al.*, 2017).

Locomotion assay

Aliquots of 10 male flies per genotype were collected the day of eclosion and transferred to a new vial containing standard food. Tracking was carried out the next day under constant conditions (25°C, 70% humidity, during Zeitgeber time 1–3). In brief, experimental flies were transferred to an arena without anaesthesia and were allowed to acclimatize for 5 min. Tracking arenas were 37 mm in diameter and 4 mm in height, allowing flies to freely walk but not jump or fly. Next, 7-min videos (10 frames per second) were recorded using HandyAvi software (Azcendant) connected to a Logitech C525 webcam positioned directly above the centre of the arena. Locomotion was tracked using the semi-automatic machine-vision program Ctrax (v.0.5.6) (Branson *et al.*, 2009). Distances within the videos were calibrated based on arena diameter. The Ctrax output files were further analysed in Excel, to calculate total distance and average velocity. For each genotype, three biological replicates were analysed.

Cell-death staining and immunofluorescence microscopy

To detect cell death, 2-day-old male flies were kept for 18 h on standard food containing 25 mM paraquat. Brains were dissected and fixed for 30 min in 3.7% paraformaldehyde, rinsed twice in PBS and blocked for 2 h in PBS-Triton™ X-100 (0.3%, PBS-T) containing 5% normal goat serum at room temperature. Brains were incubated with the primary antibodies anti-NC82 (DSHB, 1:125) and anti-Asp175 (Cell Signaling, 1:200) for 2 days at 4°C. Brains were washed five times for 10 min in PBS-T and incubated for 2 h with secondary antibodies Alexa Fluor® 568 red mouse (Life Technologies, 1:500) and Alexa Fluor® 488 green rabbit (Invitrogen, 1:500) at room temperature. Brains were mounted in Vectashield. At least 10 images were taken per genotype with a Zeiss Axio Imager Z2 fluorescence microscope (63× magnification) with Apotome. Asp175-positive cells in a defined region of interest in the protocerebrum were counted in Fiji.

Stress induction

Individual, 2-day-old male flies were placed in 65 mm × 5 mm glass tubes (Trikinetics) containing either standard food, standard food with 25 mM paraquat to induce oxidative stress, or

5% agar dissolved in water for starvation. Survival data were recorded with the *Drosophila* Activity Monitor (DAM) system (Trikinetics), and binned in 1 h intervals with DAMFileScan software (Trikinetics). Flies were considered dead when no more activity events were recorded. For each genotype, three biological replicates and a minimum of 14 technical replicates were analysed.

To measure *Gdap2* expression levels upon stress induction, 2-day-old male flies were selected for RT-qPCR after 0 h, 3 h, 6 h and 12 h stress induction. *Gdap2* expression levels were normalized against the non-treated condition (0 h). For each genotype, four to six biological and two technical replicates were analysed.

Statistical analysis

GraphPad Prism software and the one-way analysis of variance (ANOVA) with Tukey correction for multiple testing was used to calculate significant differences. Survival curves were analysed with the Log-rank test (Mantel-Cox) in GraphPad Prism 5.0. *P*-values < 0.05 were considered to be significant.

Data availability

All exome data are available via GENESIS (https://www.genesis-app.com/). All *Drosophila* data are available upon request via the corresponding author Annette Schenck.

Results

A new clinical ARCA subtype

Patient NIJ

A now 46-year-old Dutch/Egyptian female had started to notice gait difficulties at age 34, soon accompanied by speech changes and difficulty writing. These complaints worsened slowly over time. She started to fall occasionally and had to use a walker at age 43. There were no cognitive problems or autonomic disturbances. Clinical examination at age 44 years showed normal cognition (although there was some suggestion of mental slowing); gaze-evoked nystagmus, jerky pursuit, hypermetric saccades; cerebellar dysarthria; mild leftward torticollis; ataxia on finger chase and heel-shin slide; spastic ataxic gait; lower limb hypertonia; very brisk tendon reflexes, but downgoing plantar responses; no weakness; and normal sensory examination. An MRI brain scan revealed mild cerebellar atrophy. Ophthalmological examinations were normal. Nerve conduction studies and EMG did not show evidence of a peripheral neuropathy. Laboratory testing including vitamin E, metabolic screening, albumin, cholesterol, alpha-fetoprotein, lactate, acanthocytes, copper, ceruloplasmin, and coeliac screen was normal or negative. Genetic testing for Friedreich, spinocerebellar ataxias (SCAs) 1, 2, 3, 6, 12, 14 and 17, dentatorubral-pallidoluysian atrophy, autosomal recessive spastic ataxia of Charlevoix-Saguenay and SPG7 were negative.

Patient AW

This Belgian female had an uneventful prior medical history. Her family history revealed that her brother died from a brain tumour, her father died at age 84 years and had epilepsy, her mother was alive at time of presentation without ataxia or other gait disorder at age 85 years; the patient had a healthy daughter. There was no known consanguinity in the family. First symptoms developed at the age of 38 years with mild gait imbalance that progressively worsened. Speech problems started at the age of 40. Examination at age 52 years, when she was seen first, showed a severe gait ataxia and mild pyramidal features in the form of brisk reflexes; jerky eye movements without clear nystagmus; and disturbances of short-term memory and mild behavioural changes, with a Mini-Mental State Examination (MMSE) of 25/30. A clear progression was noted in the following years with further worsening of gait resulting in the use of a walker and later wheelchair (at age 54 years). At that point, clear spasticity in the legs was evident. The patient lost the ability to walk independently by the age of 58 years and by that time cognitive decline had progressed with an MMSE of 15/30, a pronounced dysexecutive syndrome, apathy, periodic aggressive behaviour, and symptoms of depression. Speech became unintelligible around the age of 59 years. Because of progressive dysphagia, a percutaneous gastric tube was placed at the age of 62 years. By that time, the patient was mutistic and bed-ridden. She died due to infectious complications at the age of 62 years. Brain MRI at age 53 years revealed severe atrophy of the cerebellum, both vermian and hemispheric, mainly of the superior aspect, and also global cerebral atrophy (cortical and central). These alterations had clearly progressed on a second MRI 4 years later. Levels of alpha-fetoprotein, vitamin E, copper, and folic acid were normal. Screening for trinucleotide repeat expansions was negative for SCAs 1, 2, 3, 6, 7, 8, 10, 12, and 17, and for Friedreich's ataxia.

Table 1 summarizes the main phenotypic features.

Cerebellar and extra-cerebellar pathological changes

The autopsy of Patient AW was limited to the brain, which weighed 1106 g. Macroscopic examination revealed a cerebellar atrophy in combination with a mild atrophy of the pes pontis (Fig. 1A and B, arrows). The bulbus olfactorius, the tractus olfactorius and the chiasma opticum were normal. A few small atheromatous plaques were found in the basilar artery. There was a dilatation of the ventricular system on both sides but the white matter had a normal aspect and consistency. The neostriatum, the pallidum and the corpus subthalamicum were normal. On the left side, the pulvinar was small and therefore extra sampling was done at thalamic level. In the brainstem, there was a pallor of the substantia nigra and of the locus coeruleus. On transverse sections, the pes pontis had a normal size with

Table 1 Summary of genetic and clinical findings

	Patient NIJ	Patient AW
GDAP2 mutations	c.946C>T; p.(Gln316*) c.1305dup; p.(Ser436fs*36) Compound heterozygous	c.1198_1199insG; p.(His400fs*15) Homozygous
Origin	Dutch/Egyptian	Belgian
Age at onset	34 years	38 years
Presenting symptom	Gait problems	Gait problems
Course	Slowly progressive	Moderately progressive
Ataxia milestone / disease duration	3 / 12 years	4 / 24 years
Predominant clinical syndrome	Cerebellar ataxia	Cerebellar ataxia and dementia
Other neurological features	Mild spastic paraplegia Cervical dystonia	Spasticity
Cognition	Normal / mild bradyphrenia	Progressive decline with clear dementia at age 53 years
MRI brain	Cerebellar atrophy	Severe atrophy cerebellum, and global supratentorial atrophy (cortical and central)
NCS/EMG	Normal	Normal
Ophthalmological evaluation	Normal	Normal

Ataxia milestones (Klockgether *et al.*, 1998): 0, normal; 1, ataxia, but independent; 2, permanently dependent on walking aids; 3, permanently dependent on wheelchair; 4, death.

a somewhat smaller tegmentum by comparison. The pyramidal pathways were relatively small in the medulla oblongata. Vertico-frontal slicing of the cerebellum confirmed the atrophy of the cerebellar foliae the more so in the paramedian areas. There was also a minimal atrophy of the dentate nucleus.

Microscopically, pathological features were found at different levels. First, there was a cerebello-olivar atrophy with a severe and diffuse loss of Purkinje cells, with an increase of the Bergmann cells and also of the glial cells present in the molecular layer (Fig. 1C and D). Some remaining Purkinje cells showed a staghorn aspect of the dendritic tree. The involvement of the inner granular layer of the cerebellar foliae was less severe. There was a relative sparing of the flocculo-nodular lobus (archicerebellum). The paleocerebellum was more affected than the neocerebellum. There were neuronal losses and astrocytic gliosis in the parvocellular part of the dentate nucleus. In the medulla oblongata, the inferior olivary nucleus showed neuronal loss more pronounced at the level of the dorsal laminae (Fig. 1E and F). The griseum pontis was normal and the brachia pontis were normally myelinated. Second, upon examination of the thalamus on both sides and at different levels, there was neuronal loss and astrocytic gliosis in the nucleus anterior, the nucleus dorsalis posterior and in the pulvinar medialis more than the lateralis (Fig. 1G and H). The lesions did not affect the nuclei according to a strict neuroanatomical pattern. There was also a vacuolation of the neurons in the magnocellular part of the nucleus centralis. Third, we observed neuronal losses in the zona compacta of the substantia nigra with a mild status pigmentatus (Fig. 1I and J), while the locus coeruleus was within normal limits. Fourth, with regard to the motor system, pallor of the pyramidal pathways in the medulla oblongata and loss of neurons in the hypoglossal nucleus was evident.

With immunohistochemistry, a few neuronal and glial cytoplasmic inclusions immunoreactive for ubiquitin and p62 (both antibodies were used to detect disturbances in ubiquitine proteasome degradation) were found in the neocortex, the hippocampus (including the gyrus dentatus), the hippocampus, the subiculum, the superficial layers of the gyrus parahippocampalis, the amygdala, the nucleus accumbens, and the corpus subthalamicum. They were few in number in the thalamic nuclei except for the magnocellular part of the nucleus centralis. Using a semi-quantitative scale (0, none; 1+, sparse; 2+, moderate; 3+, large amounts of neuronal and glial cytoplasmic inclusions), we obtained 1+ in all locations. There were no TDP-43 immunoreactive inclusions except for sparse amounts (1+) in the amygdala and the nucleus accumbens (Mackenzie *et al.*, 2011). There were neither Lewy bodies nor Lewy neurites with the anti-alpha-synuclein antibody. The 1C2 antibody used to detect trinucleotide repeat expansions, failed to reveal any neuronal intranuclear inclusions. Large amounts of AT8 immunoreactive neurofibrillary tangles, neuropil threads and dystrophic neurites were exclusively found in the hippocampus and the amygdala corresponding to a stadium III of Braak and Braak (1991) while amyloid deposits and senile plaques of all types were wholly absent.

Exome sequencing identifies variants in *GDAP2*

Exome sequencing for proband Patients NIJ and AW revealed no pathogenic mutation in known genes associated with cerebellar ataxia. Because of the sporadic nature of the cerebellar ataxia in both probands, the most likely inheritance pattern was either *de novo* autosomal dominant or autosomal recessive. Trio-sequencing analysis to detect putative *de novo* variants was not possible because of the unavailability of paternal DNA for Patient NIJ and

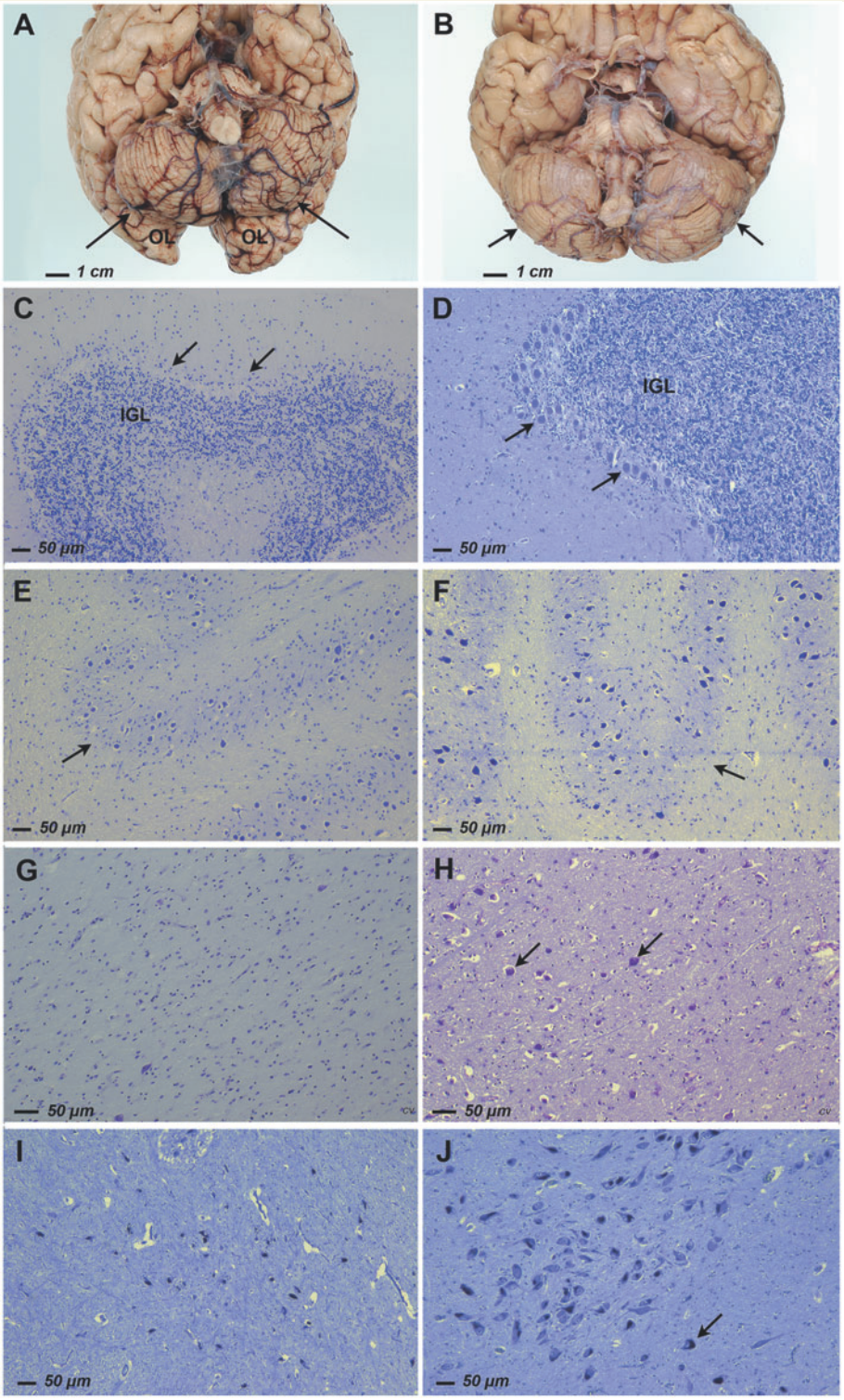

Figure 1 Main neuropathological changes within the brain of Patient AW. (**A**) Severe cerebellar atrophy (arrows) showing that a large part of the occipital lobes (OL) is not covered by the cerebellum as usual. (**B**) Control showing a normal cerebellum (arrows) covering the occipital lobes. (**C**) Cerebellar foliae showing the disappearance of the Purkinje cells (the arrows point to the layer where Purkinje cells should be). Thinning of the inner granular layer (IGL). (**D**) Control case showing the layer of the Purkinje cells (arrows) and the inner granular layer. (**E**) Dorsal part of the main olivary nucleus in the medulla oblongata (arrow). A comparison with a control case (**F**) highlights a slight loss and an atrophy of the neurons. (**F**) Control case showing larger and more numerous neurons in the same area. (**G**) Neuronal losses in the thalamic pulvinar. (**H**) Normal amounts of neurons (arrows) in a control pulvinar. (**I**) Neuronal loss and atrophy in the zona compacta of the substantia nigra. (**J**) Control case. The arrow points towards one of the many melanin-containing neurons. (**C**–**J**) Paraffin sections, cresyl violet staining. Scale bars = 50 µm.

parental DNA for Patient AW. Patient NIJ has a Dutch mother and an Egyptian father, suggesting that compound heterozygosity for a novel gene would be a plausible cause of the ataxia in this patient. The most likely candidate gene was *GDAP2*, bearing two putative loss-of-function mutations, a nonsense mutation [NM_017686.3:c.946C>T; p.(Gln316*)] and a frameshift mutation [NM_017686.3:c.1305dup; p.(Ser436fs*36)]. Analysis of the maternal DNA revealed that she carries the p.Gln316* mutation, but not the frameshift mutation, indicating that the mutations in the proband are on opposite alleles.

Independently, analysis of mutations likely involved in recessive inheritance for Patient AW revealed a damaging homozygous *GDAP2* frameshift mutation [NM_017686.3:c.1198_1199insG; p.(His400fs*15)] as the most likely causal mutation. The variant and its segregation were confirmed in the proband and her daughter using standard Sanger sequencing methodology. There was no known consanguinity in the family, but because of the small size of this kinship this could not be studied further.

Thus, biallelic mutations in *GDAP2* were identified as most likely disease-causing independently in both patients.

The three variants found are all likely loss-of-function alleles. The transcripts encoding the nonsense mutation p.(Gln316*) and the frameshift mutation p.(His400fs*15) are likely to undergo nonsense-mediated decay, since they lead to premature termination codons (PTCs) located in the exons 8 and 11 (of the 14 exons of *GDAP2* gene), respectively. The frameshift mutation p.(Ser436fs*36) results in a PTC 36 codons downstream in the penultimate exon. This PTC is only 33 bases from the 3′ end of the penultimate exon, and may thus escape nonsense-mediated decay. Nevertheless, it is expected to disrupt gene function since it changes the amino acid sequence and length of the C-terminus of the GDAP2 protein by replacing the 62 most C-terminal amino acids by 35 others, damaging the CRAL-TRIO domain, a protein structural domain that binds small lipophilic molecules (Panagabko *et al.*, 2003). The large change of the C-terminus may also destabilize the protein and trigger degradation pathways involved in protein quality control.

Additionally, no homozygous loss-of-function *GDAP2* mutations were identified in controls, while heterozygous loss-of-function variants were present in low allele frequencies only (Lek *et al.*, 2016). One of the mutations described here, p.(Gln316*), was detected with an allele frequency of 0.00008396 only, whereas the other two mutations, p.(Ser436fs*36) and p.(His400fs*15), were not observed.

Drosophila GDAP2 knockdown models

To gain independent support for the implication of GDAP2 in ARCA pathology, we turned to the fruit fly *Drosophila melanogaster*, a well established organism to model degenerative movement disorders including cerebellar ataxia (Petersen *et al.*, 2013; Dubos *et al.*, 2015; Ishiguro *et al.*, 2017). *Drosophila* contains a previously uncharacterized one-to-one orthologue of GDAP2, CG18812, hereafter referred to as *Drosophila* Gdap2 (Aken *et al.*, 2016). *Drosophila* Gdap2 shares 38% of overall sequence identity at the amino acid level, but is particularly highly conserved compared to human in the macro and CRAL-TRIO domains (73% and 68%, respectively) (Fig. 2A). The protein is broadly expressed, and expression levels are highest during late larval/early pupal stages (Celniker *et al.*, 2009; Robinson *et al.*, 2013).

We modelled loss of human GDAP2 expression by inducing ubiquitous knockdown in *Drosophila* using the UAS-Gal4 system (Brand and Perrimon, 1993), the ubiquitous promoter line Act-Gal4, and two independent UAS-RNAi lines (vdrc39224 and vdrc100622) targeting non-overlapping regions of the gene. Knockdown efficiency was enhanced by an additional copy of UAS-Dicer-2 (Dietzl *et al.*, 2007). The efficiency of ubiquitous *Gdap2* knockdown was determined by qPCR on whole fly bodies. Relative mRNA expression of *Gdap2* upon knockdown was 30% ($P < 0.01$) for Gdap2 RNAi-1 and 36% ($P < 0.001$) for Gdap2 RNAi-2, compared to their respective controls (Fig. 2B).

Drosophila Gdap2 knockdown results in decreased lifespan

Induction of ubiquitous Gdap2 knockdown, using Gdap2 RNAi-1 or Gdap2 RNAi-2, was partial lethal during metamorphosis (Fig. 2C). Male escapers were carefully monitored for defects in lifespan. Gdap2 knockdown with either Gdap2 RNAi-1 or Gdap2 RNAi-2 significantly decreased lifespan (Fig. 2D). Compared to their genetic controls with a median survival time of 46 days and 49 days, median survival time of Gdap2 RNAi-1 and Gdap2 RNAi-2 knockdown animals decreased to 22 days (0.48 relative survival time) and 9 days (0.18 relative survival time), respectively (Fig. 2D).

Drosophila Gdap2 knockdown impairs locomotor behaviour

We next inspected Gdap2 knockdown models for behavioural anomalies. We noticed that Gdap2 knockdown *Drosophila* exhibited righting defects and uncoordinated walking behaviour (Supplementary Video 1). To evaluate the possible effect of Gdap2 knockdown on further aspects of locomotor behaviour, we subjected the Gdap2 knockdown animals to the island assay. In this assay, flies are thrown onto an elevated platform. This induces an innate motor behaviour enabling healthy flies to initiate flight and escape from the platform within seconds (Schmidt *et al.*, 2012; Kochinke *et al.*, 2016; Eidhof *et al.*, 2017). Ubiquitous Gdap2 knockdown significantly decreased the ability of flies to leave the platform, compared to their

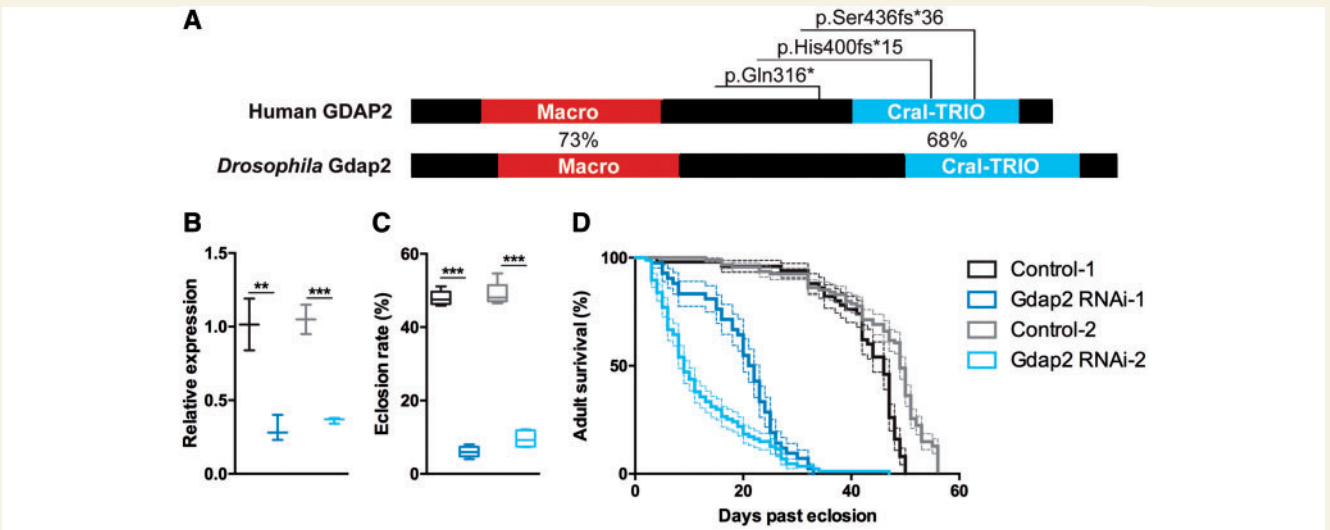

Figure 2 Modelling loss of GDAP2 function in *Drosophila* decreases survival. (**A**) High conservation of protein organization and amino acid sequence between human GDAP2 and *Drosophila* Gdap2. Conserved protein domains include the macro (red, 73% similarity) and CRAL-TRIO (blue, 68% similarity) domain. (**B**) Relative *Gdap2* expression in male Control-1 (dark grey, genotype: *UAS-Dicer-2;Actin-Gal4/+*), Gdap2 RNA-1 (dark blue, genotype: *UAS-Dicer-2;Actin-Gal4/+;Gdap2 RNAi-1/+*), Control-2 (light grey, genotype: *UAS-Dicer-2;Actin-Gal4/+*) and Gdap2 RNAi-2 (light blue, genotype: *UAS-Dicer-2;Actin-Gal4/Gdap2 RNAi-2*) flies determined by qPCR. Min-to-max boxplots represent three independent biological replicates. $^{**}P < 0.01$, $^{***}P < 0.001$. (**C** and **D**) Colour code as in **B** and in legend on the right. (**C**) Eclosion rate (in %) of Control-1, Gdap2 RNA-1, Control-2 and Gdap2 RNAi-2 male flies. Min-to-max boxplots represent three independent biological replicates. $^{***}P < 0.001$. (**D**) Kaplan Meijer curve showing survival (in %) over days past eclosion of male Control-1, Gdap2 RNA-1, Control-2 and Gdap2 RNAi-2 flies. Error bars indicate standard error (SE). *Gdap2* knockdown dramatically diminishes survival. The log-rank (Mantel-Cox) test confirmed that survival significantly differs (Control-1 versus Gdap2 RNAi-1: $P < 0.001$ and Control-2 versus Gdap2 RNAi-2: $P < 0.001$).

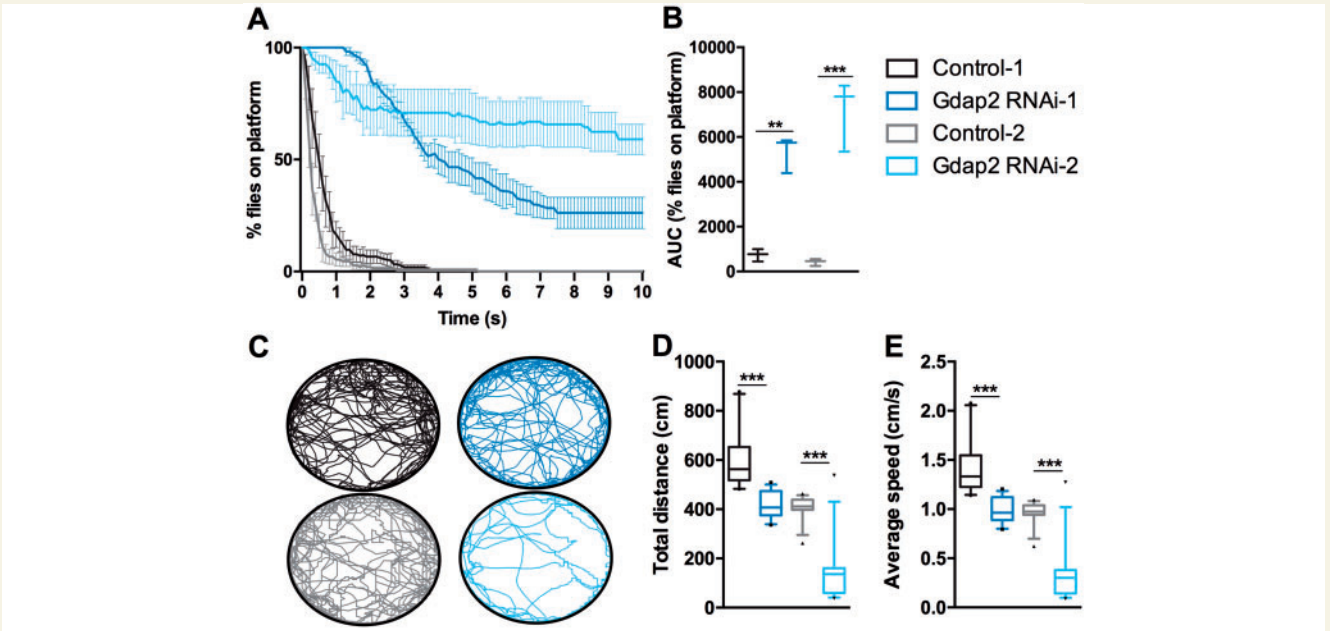

Figure 3 *Drosophila* GDAP2 knockdown models show aberrant locomotor behaviour. (**A**) *Drosophila* escape response, assessed in the island assay. Graphs show per cent of flies that remain on the platform over time (10 s). Two-day-old male Control-1 (dark grey), Gdap2 RNA-1 (dark blue), Control-2 (light grey) and Gdap2 RNAi-2 (light blue) flies were tested. Plotted is average and SEM of three independent biological replicates. (**B**) Floating bars depicting minimum, maximum and mean area under curve based on the graphs shown in **A**, $^{**}P < 0.01$, $^{***}P < 0.001$. (**C**) Locomotion trajectories of representative flies of the same genotypes as in **A** and **B**. Two-day-old male flies were recorded for 7 min at 10 frames per second in a circular arena. (**D**) Total distance (in cm) of walk in the 7 min of locomotion tracking. (**E**) Average speed (in cm/s) of the indicated genotypes during the 7 min of locomotion tracking. Genotypes are specified in the Fig. 2 legend and in the 'Materials and methods' section. Min-to-max boxplots represent data of three independent biological replicates, $^{***}P < 0.001$.

genetic background controls (Fig. 3A and B). Whereas control animals had escaped the platform within 5 s, 34% of Gdap2 RNAi-1 and 67% of Gdap2 RNAi-2 animals were left on the platform after 10 s (Fig. 3A). Gdap2 knockdown flies mostly walked over and off the platform, indicating their inability to fly away. In agreement with this, Gdap2 RNAi-1 *Drosophila* held their wings in a droopy posture in contrast to the normal wing posture of their genetic controls (Supplementary Fig. 1). We next monitored locomotor behaviour in Gdap2 knockdown models by tracing their locomotor paths over time in an open-field arena. Both RNAi lines showed reduced walking distance and speed (Fig. 3C–E). Thus, Gdap2 knockdown in *Drosophila* results in motor phenotypes.

Loss of Gdap2 increases susceptibility to oxidative stress and starvation

No information is available about GDAP2 function in any organism. However, proteins containing macro or lipid-binding CRAL-TRIO domains have been linked to many important cellular processes such as signal transduction pathways, DNA repair, necrosis, apoptosis, cell differentiation and proliferation, and intracellular trafficking (Karras *et al.*, 2005; Bankaitis *et al.*, 2010; Han *et al.*, 2011). All these processes are essential for a proper equilibrium between cellular stress, survival and death and have been implicated in neurodegenerative diseases, including ARCAs (Lim *et al.*, 2006; Sharma *et al.*, 2014; Smeets and Verbeek, 2014; Didonna and Opal, 2016). Maintaining these equilibriums and adaptation to cellular stress is, among others, dependent on changes in gene expression (Borch Jensen *et al.*, 2017). We considered the possibility that *Gdap2* could be a stress-responsive gene and investigated differential *Gdap2* expression in control strains after induction of two types of cellular stress: paraquat to induce oxidative stress (Castello *et al.*, 2007) or nutrient depletion to induce starvation. *Gdap2* mRNA levels were consistently downregulated for both Control-1 and Control-2 flies after starvation and paraquat induction (Fig. 4A–D). Relative *Gdap2* mRNA expression levels for both control strains significantly decreased to 70% or less after 3 h starvation and remained on similar levels after 6 h and 12 h starvation (Fig. 4A and B). Relative *Gdap2* mRNA expression levels for both control strains significantly decreased to 80% or less after 6 h paraquat treatment and continued to decrease significantly to 50% or less after 12 h paraquat treatment (Fig. 4C and D). Because *Gdap2* expression levels responded to cellular stress, we next asked whether reduced *Gdap2* expression levels may increase the susceptibility to deleterious effects of starvation and paraquat treatment. Treated control strains lived significantly shorter compared to non-treated control and Gdap2 knockdown flies after starvation and paraquat treatment (Fig. 4E–H). Importantly, Gdap2 knockdown flies, characterized by reduced *Gdap2* expression levels already in non-treated conditions, lived significantly shorter upon exposure to nutrient starvation and, dramatically, to paraquat, compared to treated controls (Fig. 4E–H). The median survival time of Gdap2 knockdown animals during starvation compared to starved controls was slightly lower (45 h versus 49 h, 0.92 relative survival time in Gdap2 RNAi-1 animals; 37 h versus 48 h, 0.77 relative survival time in Gdap2 RNAi-2 animals) (Fig. 4E–F). The median survival time of Gdap2 knockdown animals treated with paraquat compared to paraquat-treated controls was 26 h versus 149 h (0.17 relative survival time) in Gdap2 RNAi-1 animals and 32 h versus 156 h (0.21 relative survival time) in Gdap2 RNAi-2 animals compared to their genetic controls (Fig. 4G–H). We addressed the possibility that Gdap2 knockdown flies on paraquat die sooner due to increased levels of neurodegeneration in the central brain; however, we were not able to confirm this with cleaved-caspase-3 staining (Supplementary Fig. 2). Our results show that *Gdap2* expression levels change upon exposure to cellular stressors in control flies, and that decreased *Gdap2* expression levels in the knockdown flies increase the sensitivity against deleterious effects of oxidative stress and, to a minor degree, to nutrient deprivation. An abnormal response to cellular stress may thus contribute to the phenotypes observed in *Drosophila* GDAP2 knockdown models.

Discussion

Here, we report two unrelated individuals with compound heterozygous or homozygous gene-disruptive mutations in *GDAP2*. The main clinical theme in both individuals was cerebellar ataxia, which manifested in their fourth decade. They also developed spasticity, and dementia emerged in the patient with long follow-up time and eventual early death (Patient AW). This cognitive phenotype was paralleled by global cerebral atrophy accompanying the cerebellar atrophy on brain imaging. Neuropathological investigations confirmed clear degenerative changes in the cerebellum, but also involvement of the thalamus, substantia nigra, and pyramidal tracts that may underlie the other motor features. Using Montine's scoring system (Montine *et al.*, 2012) for amyloid deposition, neurofibrillary tangles and neuritic plaques, the low score of A0B2C0 argues against amyloid pathology as an alternative explanation of the co-emerging dementia. The AT8 immunoreactive tangles in the hippocampus and amygdala lead to a formal neuropathological diagnosis of primary age-related tauopathy (Crary *et al.*, 2014). There were not enough features to consider a diagnosis of fronto-temporal lobe degeneration-TDP type B (Mackenzie *et al.*, 2011). Other theoretical substrates for the cognitive decline could be the bilateral thalamic lesions affecting the nucleus anterior and the pulvinar, or the cerebellum. Whether and how any of these mechanisms is related to *GDAP2* mutations is unclear. Further follow-up of Patient NIJ, who is still in an earlier disease stage, and the identification of more patients with *GDAP2* mutations will allow us to further delineate the GDAP2 loss-of-function phenotypic spectrum.

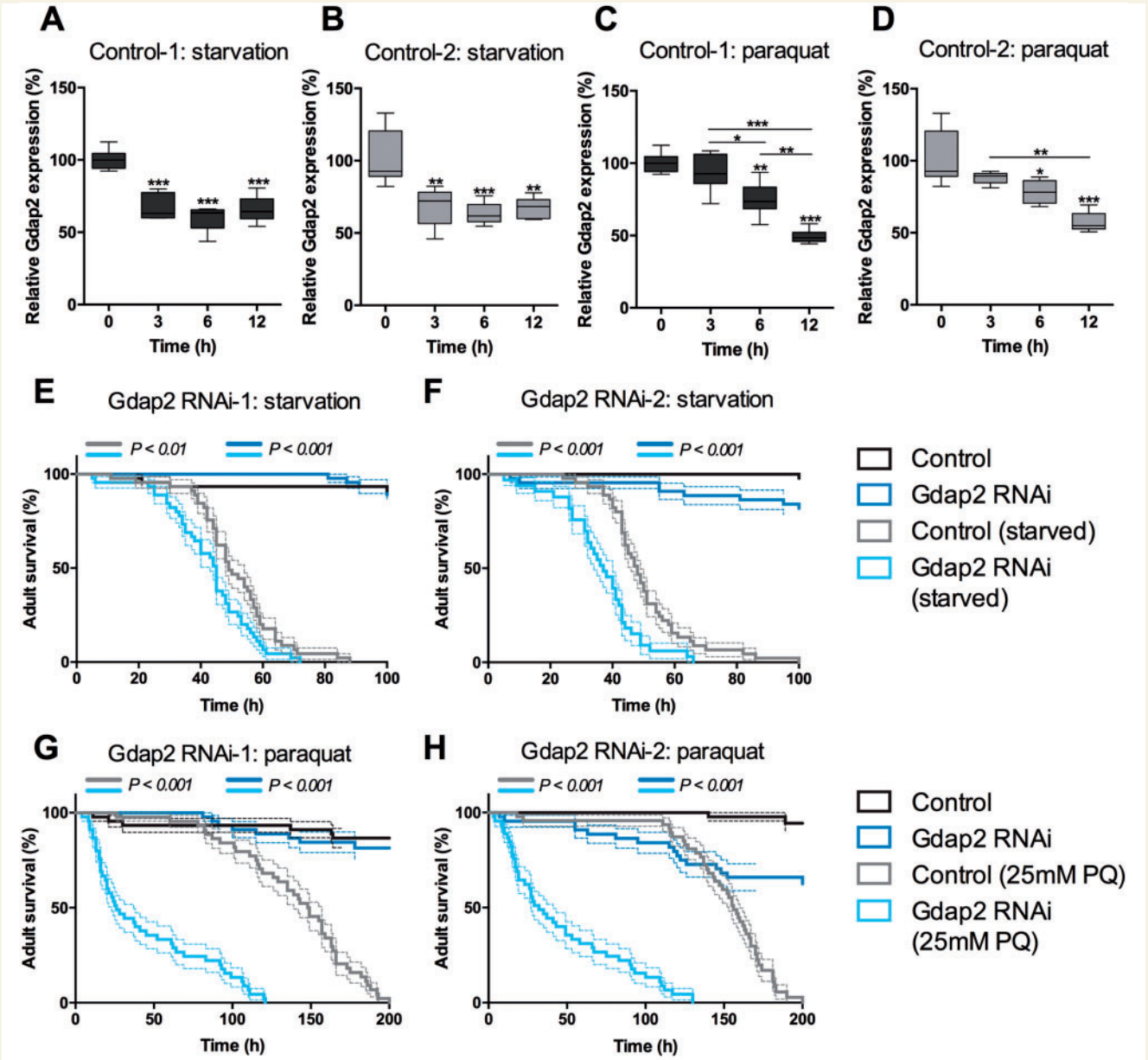

Figure 4 ***Drosophila*** **GDAP2 knockdown models are susceptible to cellular stress.** (**A**–**D**) Relative Gdap2 expression levels are reduced upon starvation (**A** and **B**) and 25 mM paraquat exposure (**C** and **D**) in two control strains. Plotted are min-to-max boxplots of 4–6 biological replicates. *$P < 0.05$, **$P < 0.01$, ***$P < 0.001$. (**E**–**H**) Kaplan Meijer curve showing survival (in %) over time upon exposure to the indicated stressors. (**E** and **F**) Starvation (starved), (**G** and **H**) oxidative stress induced by 25 mM paraquat (25 mM PQ). Male flies were tested, genetic conditions, treated (light blue or light grey lines) and untreated (dark blue or dark grey lines), are specified in the legend on the *right*. Gdap2 knockdown flies (Gdap2 RNAi-1 and RNAi-2) lived significantly shorter upon nutrient starvation (**E** and **F**) or 25 mM paraquat exposure (**G** and **H**) compared to treated controls and untreated Gdap2 knockdown and control flies. *P*-values are indicated above each panel, genotypes are specified in the Fig. 2 legend and in the 'Materials and methods' section. Error bars represent SE. Log-rank (Mantel-Cox) test was used to determine whether survival curves significantly differ from each other.

The clearly gene-disruptive nature of the mutations, absence of homozygous *GDAP2* loss-of-function mutations in controls (Lek *et al.*, 2016), and shared clinical presentation and time of onset strongly suggest that loss of GDAP2 function underlies this new ARCA subtype. As other biallelic *GDAP2* variants were absent in over 500 ataxia exomes at the Nijmegen and Miami sites, this is likely a rare cause of ARCA.

The causality of *GDAP2* gene-disruptive mutations in cerebellar and global cerebral atrophy is supported by high GDAP2 expression levels in the human brain, which were increased in the human cerebellum during postnatal stages compared to other brain regions (Supplementary Fig. 3A) and high GDAP2 expression levels in the cerebellum of mice (Supplementary Fig. 3B). Further, modelling of GDAP2 loss-of-function in *D. melanogaster*, an established

model for movement disorders, resulted in locomotor defects and shortened lifespan, supporting an evolutionary role for GDAP2 in these processes. The origin of the *Drosophila* locomotor phenotypes need further investigation. Their early onset suggests a potential developmental component, whereas disease onset in GDAP2 patients is in adulthood. Decreased genetic redundancy within gene families and between molecular pathways in fly compared to humans may disable compensatory mechanisms, potentially accounting for this difference. Indeed, *GDAP2* is part of a gene family (www.treefam.org) (Schreiber *et al.*, 2014). Moreover, numerous *Drosophila* models of other progressive neurodegenerative disorders also induce neurodevelopmental phenotypes, e.g. SCA5 (Lorenzo *et al.*, 2010), progressive myoclonus epilepsy (Ehaideb *et al.*, 2014; Praschberger *et al.*, 2017), hereditary spastic paraplegia type 30 (Kern *et al.*, 2013) and SCA with neuropathy (Dunlop *et al.*, 2004).

Although *GDAP2* molecular function and mechanisms underlying its associated neurodegenerative pathology remain elusive, important hints are provided by its gene product. *GDAP2* was previously identified as one of the 10 cDNAs upregulated during neurite sprouting of a Neuro2a mouse neuroblastoma cell line upon expression of GD3 synthase and was therefore called 'ganglioside induced differentiation associated protein 2'. GDAP1, another member of the ganglioside-induced differentiation-associated family, has been described in Charcot-Marie-Tooth disease, a degenerative peripheral nerve disorder, which may suggest a conserved role of GDAP proteins in neuronal maintenance and locomotor function. In spite of this, little similarity exists between GDAP2 and GDAP1 amino acid sequences (<2%).

The GDAP2 protein contains a unique combination of functional domains: a macro and a CRAL-TRIO domain (Aken *et al.*, 2016). Only 11 macro domain-containing proteins exist in humans. The macro domain of GDAP2 is very similar to that of MacroD1/MacroD2 proteins, but has little affinity for nicotinamide adenine dinucleotide (NAD+)-derived metabolites; it has poly(A) affinity instead (Neuvonen and Ahola, 2009). Overall, macro domain-containing proteins have been described as sensors of cellular metabolic states and are involved in cellular redox homeostasis, DNA damage and repair, the formation of cytosolic stress granules that can protect mRNAs from degradation, apoptosis, and necrosis (Karras *et al.*, 2005; Han *et al.*, 2011; Posavec *et al.*, 2013; Leung, 2014; Gonzalez Esquivel *et al.*, 2017). Although it is not clear whether GDAP2 operates in these processes, it is noticeable that defects in these key pathways have been linked to many neurodegenerative disorders, including ARCAs (Lim *et al.*, 2006; Barclay *et al.*, 2014; Sharma *et al.*, 2014; Smeets and Verbeek, 2014; Didonna and Opal, 2016). The CRAL-TRIO domain is a lipid-binding domain, and CRAL-TRIO-domain-only proteins are involved in lipid transport. Of note, CRAL-TRIO domains have been found in other genes causing ARCAs when mutated, including ataxia with vitamin E deficiency (AVED) caused by defects in α-TTP, and Cayman ataxia with loss of function of the caytaxin protein (Schuelke, 1993; Bomar *et al.*, 2003). Multi-domain CRAL-TRIO containing proteins, such as GDAP2, are thought to have more complex functions in signal transduction, transport, and organelle biology, where they integrate lipid metabolism with other biochemical processes (Saito *et al.*, 2007). This information suggests that GDAP2 might be involved in cellular metabolic and/or stress responses. In line with this, we demonstrated that in *Drosophila Gdap2* expression significantly decreases after stress induction in wild-type animals and that Gdap2 knockdown increases the sensitivity to deleterious effects of oxidative stress and, to a minor degree, to nutrient deprivation. Since Gdap2 knockdown flies also show shortened lifespan in non-stressed conditions, we considered the possibility that the decreased lifespan of Gdap2 knockdown flies upon stress are additive effects. However, *Gdap2* expression levels directly responded to stress exposure in wild-type animals. Also, the effect of the paraquat stressor, exerting a milder effect on the lifespan in controls, was very dramatic in Gdap2 knockdown flies compared to the more severe nutrient deprivation stressor. We therefore propose that at least the high susceptibility to paraquat goes beyond an additive effect. After 18-h paraquat induction, we were unable to show increased levels of apoptosis in the brains of GDAP2 knockdown models compared to genetic controls. This suggests that the decreased lifespan of the GDAP2 knockdown models upon stress might, at this stage, be a consequence of neuronal dysfunction instead of neuronal degeneration. This is supported by data from other genetic ataxias suggesting that neuronal dysfunction indeed precedes neuronal degeneration (Dell'Orco *et al.*, 2015). Alternatively, fly brains would also need to be tested directly after organismal death, or the time window of stress induction that we tested may not be long enough to observe neuronal degeneration accumulating. Because of the strong deleterious of 25 mM paraquat on lifespan, additional experimental series with milder stressors may be more informative. Altered responses to cellular stress may thus reflect a direct role of GDAP2 in stress conditions.

Gdap2 could be functioning in key homeostatic metabolic processes that are downregulated during cellular stress, to ensure proper activation or action of proteins protecting against stress. Prolonged downregulation of these processes might affect neuronal functioning and could be deleterious. An alternative explanation for our findings could be that decreased *Gdap2* expression levels upon stress could be a deleterious consequence of the stressor and part of the damaging process. Reduced levels of *Gdap2* prior to the stressor would then cause even faster or more severe damage. Further research is required to examine these primary inferences on the exact function of Gdap2. In both scenarios, however, stress susceptibility may contribute to the phenotypes observed in the

Drosophila GDAP2 knockdown models and in individuals with biallelic *GDAP2* mutations.

In summary, we define a new subtype of ARCA caused by gene-disruptive mutations in the *GDAP2* gene. The corresponding *Drosophila* model suggests that GDAP2 is an evolutionary conserved, potentially stress-dependent regulator that, when mutated, affects motor behaviour and lifespan.

Acknowledgements

We acknowledge the Genome Technology Center at the Radboud UMC and the Beijing Genome Institute Europe (Copenhagen, Denmark) for their exome sequencing services. We acknowledge the Vienna *Drosophila* Resource Center and Bloomington *Drosophila* stock centre for providing *Drosophila* strains. We thank M. Coll-Tané for genotyping the insertion site of vdrc100622 and the Cold Spring Harbor *Drosophila* Neurobiology: Genes, Circuits and Behavior course for expert support.

Funding

This research was supported by the E-RARE-3 Joint Transnational Call grant "Preparing therapies for autosomal recessive ataxias" (PREPARE; ZonMW, 9003037604 to A.S. and B.v.d.W.), by a Radboud university medical centre junior researcher grant to B.v.d.W. and A.S., the E-Rare Network NEUROLIPID (01GM1408B to R.S.), the US National Institutes of Health (NIH) (grants 5R01NS072248 and U54NS092091 to R.S.), by the Association Belge contre les Maladies Neuromusculaires (ABMM) - Aide à la Recherche ASBL, and the EU FP7/2007-2013 under grant agreement number 2012-305121 (NEUROMICS). J.B. is supported by a Senior Clinical Researcher mandate of the Research Fund - Flanders (FWO). BPvdW is supported by research grants from Radboud university medical centre, ZonMW, Hersenstichting, and Bioblast Pharma.

Competing interests

The authors report no competing interests.

Supplementary material

Supplementary material is available at *Brain* online.

References

Aken BL, Ayling S, Barrell D, Clarke L, Curwen V, Fairley S, et al. The Ensembl gene annotation system. Database 2016; 2016: baw093.

Anheim M, Tranchant C, Koenig M. The autosomal recessive cerebellar ataxias. N Engl J Med 2012; 366: 636–46.

Bankaitis VA, Mousley CJ, Schaaf G. The Sec14 superfamily and mechanisms for crosstalk between lipid metabolism and lipid signaling. Trends Biochem Sci 2010; 35: 150–60.

Barclay SS, Tamura T, Ito H, Fujita K, Tagawa K, Shimamura T, et al. Systems biology analysis of Drosophila in vivo screen data elucidates core networks for DNA damage repair in SCA1. Hum Mol Genet 2014; 23: 1345–64.

Bomar JM, Benke PJ, Slattery EL, Puttagunta R, Taylor LP, Seong E, et al. Mutations in a novel gene encoding a CRAL-TRIO domain cause human Cayman ataxia and ataxia/dystonia in the jittery mouse. Nat Genet 2003; 35: 264–9.

Borch Jensen M, Qi Y, Riley R, Rabkina L, Jasper H. PGAM5 promotes lasting FoxO activation after developmental mitochondrial stress and extends lifespan in Drosophila. Elife 2017; 6: e37316.

Braak H, Braak E. Neuropathological stageing of Alzheimer-related changes. Acta Neuropathol 1991; 82: 239–59.

Brand AH, Perrimon N. Targeted gene expression as a means of altering cell fates and generating dominant phenotypes. Development 1993; 118: 401–15.

Branson K, Robie AA, Bender J, Perona P, Dickinson MH. High-throughput ethomics in large groups of Drosophila. Nat Methods 2009; 6: 451–7.

Castello PR, Drechsel DA, Patel M. Mitochondria are a major source of paraquat-induced reactive oxygen species production in the brain. J Biol Chem 2007; 282: 14186–93.

Celniker SE, Dillon LA, Gerstein MB, Gunsalus KC, Henikoff S, Karpen GH, et al. Unlocking the secrets of the genome. Nature 2009; 459: 927–30.

Crary JF, Trojanowski JQ, Schneider JA, Abisambra JF, Abner EL, Alafuzoff I, et al. Primary age-related tauopathy (PART): a common pathology associated with human aging. Acta Neuropathol 2014; 128: 755–66.

Dell'Orco JM, Wasserman AH, Chopra R, Ingram MA, Hu YS, Singh V, et al. Neuronal atrophy early in degenerative ataxia is a compensatory mechanism to regulate membrane excitability. J Neurosci 2015; 35: 11292–307.

Didonna A, Opal P. Advances in sequencing technologies for understanding hereditary ataxias: a review. JAMA Neurol 2016; 73: 1485–90.

Dietzl G, Chen D, Schnorrer F, Su KC, Barinova Y, Fellner M, et al. A genome-wide transgenic RNAi library for conditional gene inactivation in *Drosophila*. Nature 2007; 448: 151–6.

Dubos A, Castells-Nobau A, Meziane H, Oortveld MA, Houbaert X, Iacono G, et al. Conditional depletion of intellectual disability and Parkinsonism candidate gene ATP6AP2 in fly and mouse induces cognitive impairment and neurodegeneration. Hum Mol Genet 2015; 24: 6736–55.

Dunlop J, Morin X, Corominas M, Serras F, Tear G. glaikit is essential for the formation of epithelial polarity and neuronal development. Curr Biol 2004; 14: 2039–45.

Ehaideb SN, Iyengar A, Ueda A, Iacobucci GJ, Cranston C, Bassuk AG, et al. prickle modulates microtubule polarity and axonal transport to ameliorate seizures in flies. Proc Natl Acad Sci USA 2014; 111: 11187–92.

Eidhof I, Fenckova M, Elurbe DM, van de Warrenburg B, Castells Nobau A, Schenck A. High-throughput analysis of locomotor behavior in the *Drosophila* island assay. J Vis Exp 2017; 129: 1–11.

Gonzalez Esquivel D, Ramirez-Ortega D, Pineda B, Castro N, Rios C, Perez de la Cruz V. Kynurenine pathway metabolites and enzymes involved in redox reactions. Neuropharmacology 2017; 112 (Pt B): 331–45.

Gonzalez M, Falk MJ, Gai X, Postrel R, Schule R, Zuchner S. Innovative genomic collaboration using the GENESIS (GEM.app) platform. Hum Mutat 2015; 36: 950–6.

Gonzalez MA, Lebrigio RF, Van Booven D, Ulloa RH, Powell E, Speziani F, et al. GEnomes Management Application (GEM.app): a new software tool for large-scale collaborative genome analysis. Hum Mutat 2013; 34: 842–6.

Green EW, Fedele G, Giorgini F, Kyriacou CP. A Drosophila RNAi collection is subject to dominant phenotypic effects. Nat Methods 2014; 11: 222–3.

Han W, Li X, Fu X. The macro domain protein family: structure, functions, and their potential therapeutic implications. Mutat Res 2011; 727: 86–103.

Ishiguro T, Sato N, Ueyama M, Fujikake N, Sellier C, Kanegami A, et al. Regulatory Role of RNA Chaperone TDP-43 for RNA Misfolding and Repeat-Associated Translation in SCA31. Neuron 2017; 94: 108–24.e7.

Karras GI, Kustatscher G, Buhecha HR, Allen MD, Pugieux C, Sait F, et al. The macro domain is an ADP-ribose binding module. EMBO J 2005; 24: 1911–20.

Kern JV, Zhang YV, Kramer S, Brenman JE, Rasse TM. The kinesin-3, unc-104 regulates dendrite morphogenesis and synaptic development in Drosophila. Genetics 2013; 195: 59–72.

Klockgether T, Ludtke R, Kramer B, Abele M, Burk K, Schols L, et al. The natural history of degenerative ataxia: a retrospective study in 466 patients. Brain 1998; 121 (Pt 4): 589–600.

Kochinke K, Zweier C, Nijhof B, Fenckova M, Cizek P, Honti F, et al. Systematic phenomics analysis deconvolutes genes mutated in intellectual disability into biologically coherent modules. Am J Hum Genet 2016; 98: 149–64.

Lek M, Karczewski KJ, Minikel EV, Samocha KE, Banks E, Fennell T, et al. Analysis of protein-coding genetic variation in 60 706 humans. Nature 2016; 536: 285–91.

Leung AK. Poly(ADP-ribose): an organizer of cellular architecture. J Cell Biol 2014; 205: 613–19.

Lim J, Hao T, Shaw C, Patel AJ, Szabo G, Rual JF, et al. A protein-protein interaction network for human inherited ataxias and disorders of Purkinje cell degeneration. Cell 2006; 125: 801–14.

Lorenzo DN, Li MG, Mische SE, Armbrust KR, Ranum LP, Hays TS. Spectrin mutations that cause spinocerebellar ataxia type 5 impair axonal transport and induce neurodegeneration in Drosophila. J Cell Biol 2010; 189: 143–58.

Mackenzie IR, Neumann M, Baborie A, Sampathu DM, Du Plessis D, Jaros E, et al. A harmonized classification system for FTLD-TDP pathology. Acta Neuropathol 2011; 122: 111–13.

Montine TJ, Phelps CH, Beach TG, Bigio EH, Cairns NJ, Dickson DW, et al. National Institute on Aging-Alzheimer's Association guidelines for the neuropathologic assessment of Alzheimer's disease: a practical approach. Acta Neuropathol 2012; 123: 1–11.

Mukhopadhyay A, Kramer JM, Merkx G, Lugtenberg D, Smeets DF, Oortveld MA, et al. CDK19 is disrupted in a female patient with bilateral congenital retinal folds, microcephaly and mild mental retardation. Hum Genet 2010; 128: 281–91.

Neuvonen M, Ahola T. Differential activities of cellular and viral macro domain proteins in binding of ADP-ribose metabolites. J Mol Biol 2009; 385: 212–25.

Neveling K, Feenstra I, Gilissen C, Hoefsloot LH, Kamsteeg EJ, Mensenkamp AR, et al. A post-hoc comparison of the utility of sanger sequencing and exome sequencing for the diagnosis of heterogeneous diseases. Hum Mutat 2013; 34: 1721–6.

Panagabko C, Morley S, Hernandez M, Cassolato P, Gordon H, Parsons R, et al. Ligand specificity in the CRAL-TRIO protein family. Biochemistry 2003; 42: 6467–74.

Petersen AJ, Katzenberger RJ, Wassarman DA. The innate immune response transcription factor relish is necessary for neurodegeneration in a Drosophila model of ataxia-telangiectasia. Genetics 2013; 194: 133–42.

Posavec M, Timinszky G, Buschbeck M. Macro domains as metabolite sensors on chromatin. Cell Mol Life Sci 2013; 70: 1509–24.

Praschberger R, Lowe SA, Malintan NT, Giachello CNG, Patel N, Houlden H, et al. Mutations in Membrin/GOSR2 reveal stringent secretory pathway demands of dendritic growth and synaptic integrity. Cell Rep 2017; 21: 97–109.

Robinson SW, Herzyk P, Dow JA, Leader DP. FlyAtlas: database of gene expression in the tissues of Drosophila melanogaster. Nucleic Acids Res 2013; 41: D744–50.

Saito K, Tautz L, Mustelin T. The lipid-binding SEC14 domain. Biochim Biophys Acta 2007; 1771: 719–26.

Schmidt I, Thomas S, Kain P, Risse B, Naffin E, Klambt C. Kinesin heavy chain function in Drosophila glial cells controls neuronal activity. J Neurosci 2012; 32: 7466–76.

Schreiber F, Patricio M, Muffato M, Pignatelli M, Bateman A. TreeFam v9: a new website, more species and orthology-on-the-fly. Nucleic Acids Res 2014; 42: D922–5.

Schuelke M. Ataxia with vitamin E deficiency. In: Pagon RA, Adam MP, Ardinger HH, Wallace SE, Amemiya A, Bean LJH, et al., editors. GeneReviews(R). Seattle, WA: NCBI; 1993.

Sharma NK, Lebedeva M, Thomas T, Kovalenko OA, Stumpf JD, Shadel GS, et al. Intrinsic mitochondrial DNA repair defects in Ataxia Telangiectasia. DNA Repair (Amst) 2014; 13: 22–31.

Smeets CJ, Verbeek DS. Cerebellar ataxia and functional genomics: Identifying the routes to cerebellar neurodegeneration. Biochim Biophys Acta 2014; 1842: 2030–8.

Synofzik M, Smets K, Mallaret M, Di Bella D, Gallenmuller C, Baets J, et al. SYNE1 ataxia is a common recessive ataxia with major non-cerebellar features: a large multi-centre study. Brain 2016; 139 (Pt 5): 1378–93.

van de Warrenburg BP, Schouten MI, de Bot ST, Vermeer S, Meijer R, Pennings M, et al. Clinical exome sequencing for cerebellar ataxia and spastic paraplegia uncovers novel gene-disease associations and unanticipated rare disorders. Eur J Hum Genet 2016; 24: 1460–6.

Vissers JH, Manning SA, Kulkarni A, Harvey KF. A Drosophila RNAi library modulates Hippo pathway-dependent tissue growth. Nat Commun 2016; 7: 10368.